Theory of two-photon absorption in poly(diphenyl) polyacetylenes

Alok Shukla

Physics Department, Indian Institute of Technology, Powai, Mumbai 400076 INDIA

Abstract

In this paper, we present a theoretical study of the nonlinear optical response of the newly discovered conjugated polymer poly(diphenyl)polyacetylene (PDPA). In particular, we compute the third-order nonlinear susceptibility corresponding to two-photon absorption process in PDPA using: (a) independent-particle Hückel model, and (b) using the correlated-electron Pariser-Parr-Pople (P-P-P) model coupled with various configuration-interaction methodologies such as the singles-configuration-interaction (SCI), the multi-reference-singles-doubles CI (MRSDCI), and the quadruples-CI (QCI) method. At all levels of theory, the polymer is found to exhibit highly anisotropic nonlinear optical response, distributed over two distinct energy scales. The low-energy response is predominantly polarized in the conjugation direction, and can be explained in terms of chain-based orbitals. The high-energy response of the polymer is found to be polarized perpendicular to the conjugation direction, and can be explained in terms of orbitals based on the side phenylene rings. Moreover, the intensity of the nonlinear optical response is also enhanced as compared to the corresponding polyenes, and can be understood in terms of reduced optical gap.

Key words: conjugated polymers, nonlinear optics
two-photon absorption, electron-correlation effects
PACS: 78.30.Jw, 78.20.Bh, 42.65-k

1 Introduction

Conjugated polymers are among the prime candidates as materials for the future nonlinear opto-electronic devices[1]. The nonlinear optical response of these materials owes its origin predominantly to the π electrons which (a)

Email address: shukla@phy.iitb.ac.in (Alok Shukla).

are localized as far as motion transverse to the backbone of the polymer is concerned, but (b) are quite delocalized along the backbone of the polymer. Indeed, the theoretical studies of the nonlinear optical properties of a variety of conjugated polymers such as *trans*-polyacetylene, poly-(para)phenylene (PPP), poly-(para)phenylenevinylene (PPV) etc. have attracted considerable attention over the past years[2,3,4,5,6,7,8]. However, recently a new class of conjugated polymers called phenyl-substituted polyacetylenes have been synthesized which are obtained by substituting the side H atoms of *trans*-polyacetylene by phenyl derivatives, and their optical properties have been studied[9,10,11,12,13,14,15,16]. The polymers obtained by replacing all the side H atoms of the *trans*-polyacetylene by phenyl groups are called phenyl-disubstituted polyacetylenes (PDPA's), while the ones obtained by replacing alternate H atoms by the phenyl groups are called poly-phenylacetylenes (PPA's). Experimentally it was demonstrated that PDPA's exhibit strong photoluminescence (PL) with large quantum efficiency[11,12,13,16], while the PPA's on the other hand exhibit weak PL[15], akin to *trans*-polyacetylene. PDPA, similar to *trans*-polyacetylene, is a polymer with a degenerate ground state, therefore, strong PL exhibited by it was considered to be counterintuitive[13]. However, in a series of papers we demonstrated that the strong PL of PDPA's is due to reversed excited state ordering in these materials, as compared to *trans*-polyacetylene[17,18,19]. In *trans*-polyacetylene the two-photon state $2A_g$ occurs below the optical state $1B_u$, rendering it a poor emitter, while in PDPA's we showed that the reduced correlation effects stemming from the delocalization of electrons along the transverse directions, bring the $1B_u$ state below the $2A_g$, converting them into strong emitters[17,18,19]. We also demonstrated that due to the transverse delocalization, the optical gaps in PDPA's get lowered as compared to *trans*-polyacetylene[17,18,19]. Additionally, we predicted that another consequence of transverse delocalization will be the significant presence of the transverse polarization (y-component, if the conjugation direction is x) in the photon emitted during the PL process in PDPA's[17,18,19]. Since then, this prediction of ours has been verified in oriented thin-film based PL experiments conducted on PDPA, by Fujii et al[16].

Despite numerous investigations of the linear optics of PDPA's, so far there has neither been any theoretical, nor any experimental, investigation of the nonlinear optical properties of these materials. Intuitively it is obvious that, because of the large number of π-electrons even in small oligomers of PDPA's, these systems should exhibit large nonlinear optical response. Since PDPA's are materials which possess inversion symmetry, therefore, similar to *trans*-polyacetylene, the first nonlinear response that they will exhibit will be at the third order in the radiation field. However, unlike *trans*-polyacetylene, which has no side conjugation, the nonlinear response of PDPA's should also be significant to the y-polarized radiation, thereby rendering it anisotropic. Moreover, using linear spectroscopy, for centrosymmetric systems such as PDPA's, it is possible to explore only the excited states of B_u symmetry. However, us-

ing two-photon absorption (TPA) nonlinear spectroscopy, one can investigate A_g-type excited states, thereby shedding more light on the nature of electronic states in these systems. It is because of these reasons that we decided to undertake a systematic theoretical study of the TPA spectroscopy of PDPA oligomers. In the present paper, we consider oligo-PDPA's of varying lengths and compute their third-order nonlinear susceptibilities corresponding to the TPA process, using both the independent particle Hückel model, as well as Coulomb-correlated Pariser-Parr-Pople (P-P-P) mocel. We decided to perform both the independent-particle as well as correlated electron calculations so as to compare and contrast the predictions of both the models, as well as to understand the influence of electron-correlation effects on the nonlinear optical response of the PDPA's. For the P-P-P model calculations, we employed a configuration-interaction (CI) methodology, and approaches such as singles-CI (SCI), multi-reference-singles-doubles CI (MRSDCI), and quadruples-CI (QCI) were used to compute these spectra. We also compare computed TPA spectra on oligo-PDPA's, with those on the oligomers of *trans*-polyacetylene (polyenes) with the same number of unit cells. While performing this comparison, we pay particular attention to the "essential-states picture"[3,4] which was developed to explain the nonlinear optical response of conjugated polymers such as *trans*-polyacetylene, in terms of a small number of excited states. Despite the fact that oligo-PDPA's are much more complex in structure than polyenes, we find that the essential states picture remains valid to a large extent for these systems as well.

The remainder of this paper is organized as follows. In section 2 we briefly describe the theoretical methodology used to perform the calculations in the present work. Next in section 3 we present and discuss the calculated nonlinear optical susceptibilities of oligo-PDPA's. Finally, in section 4 we summarize our conclusions, and discuss possible directions for future work.

2 Methodology

The unit cell of PDPA oligomers considered in this work is presented in Fig. 1 Ground state geometry of PDPA's, to the best of our knowledge, is still unknown. However, from a chemical point of view, it is intuitively clear that the steric hindrance would cause a rotation of the side phenyl rings so that they would no longer be coplanar with the polyene backbone of the polymer. The extent of this rotation is also unknown, however, it is clear that the angle of rotation has to be less than 90 degrees because that would effectively make the corresponding hopping element zero, implying a virtual disconnection of the side phenyl rings from the backbone. In our previous works[17,18,19], we argued that the steric hindrance effects can be taken into account by assuming that the phenyl rings of the unit cell are rotated with respect to the y-axis by 30

A. Shukla: Fig 1

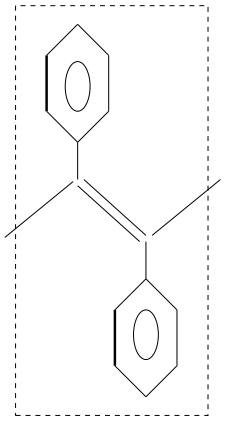

Figure 1. The unit cell of PDPA. The phenyl rings are rotated with respect to the y-axis, which is transverse to the axis of the polyene backbone (x-axis)

degrees in such a manner that the oligomers still have inversion symmetry. In the following, we will adopt the notation PDPA-n to denote a PDPA oligomer containing n unit cells of the type depicted in Fig. 1.

The point group symmetry associated with *trans*-polyacetylene (and polyenes) is C_{2h} so that the one-photon states belong to the irreducible representation (irrep) B_u, while the ground state and the two-photon excited states belong to the irrep A_g. Because of the phenyl group rotation mentioned above, the point group symmetry of PDPA's is C_i so that its ground state and the two-photon excited states belong to the irrep A_g, while the one-photon excited states belong to the irrep A_u. However, to facilitate direct comparison with polyenes, we will refer to the one-/two-photon states of PDPA's also as B_u/A_g-type states.

The independent-electron calculations on the oligomers PDPA-n were performed using the Hückel model Hamiltonian which, adopting a notation identical to our previous works[17,18,19] reads,

$$H = H_C + H_P + H_{CP}, \tag{1a}$$

where H_C and H_P are the one-electron Hamiltonians for the carbon atoms located on the *trans*-polyacetylene backbone (chain), and the phenyl groups, respectively, H_{CP} is the one-electron hopping between the chain and the phenyl units. The individual terms can now be written as,

$$H_C = -\sum_{\langle k,k'\rangle,M} (t_0 - (-1)^M \Delta t) B_{k,k';M,M+1}, \tag{1b}$$

$$H_P = -t_0 \sum_{\langle \mu,\nu\rangle,M} B_{\mu,\nu;M,M}, \tag{1c}$$

and

$$H_{CP} = -t_{\perp} \sum_{\langle k,\mu \rangle, M} B_{k,\mu;M,M,}. \tag{1d}$$

In the equation above, k, k' are carbon atoms on the polyene backbone, μ, ν are carbon atoms located on the phenyl groups, M is a unit consisting of a phenyl group and a polyene carbon, $\langle ... \rangle$ implies nearest neighbors, and $B_{i,j;M,M'} = \sum_{\sigma}(c^{\dagger}_{i,M,\sigma}c_{j,M',\sigma} + h.c.)$. Matrix elements t_0, and $t_{\perp}$ depict one-electron hops. In H_C, Δt is the bond alternation parameter arising due to electron-phonon coupling. In H_{CP}, the sum over μ is restricted to atoms of the phenyl groups that are directly bonded to backbone carbon atoms.

As far as the values of the hopping matrix elements are concerned, we took $t_0 =$ 2.4 eV, while it is imperative to take a smaller value for $t_{\perp}$, because of the twist in the corresponding bond owing to the steric hindrance mentioned above. We concluded that for a phenyl group rotation of 30 degrees, the maximum possible value of $t_{\perp}$ can be 1.4 eV[17]. Bond alternation parameter $\Delta t = 0.45$ eV was chosen so that the backbone corresponds to *trans*-polyacetylene with the optical gap of 1.8 eV in the long chain limit.

The TPA processes in oligo-PDPA's were studied by computing the third-order nonlinear susceptibilities $\chi^{(3)}(-\omega;\omega,-\omega,\omega)$. For short we will refer to these susceptibilities as $\chi^{(3)}_{TPA}$. First the Hückel Hamiltonian for the corresponding oligo-PDPA was diagonalized to compute the one-electron eigenvalues and eigenfunctions. These quantities were subsequently used in the formulas derived by Yu and Su[20], to compute $\chi^{(3)}_{TPA}$.

The correlated calculations on oligo-PDPA's were performed using the P-P-P model Hamiltonian

$$H = H_C + H_P + H_{CP} + H_{ee}, \tag{2}$$

where H_C, H_P, H_{CP} are the one-electron parts of the Hamiltonian mentioned above, while H_{ee} depicts the electron-electron repulsion and can be written as

$$\begin{aligned} H_{ee} = & U \sum_i n_{i\uparrow} n_{i\downarrow} \\ & + \frac{1}{2} \sum_{i \neq j} V_{i,j}(n_i - 1)(n_j - 1), \end{aligned} \tag{3}$$

where i and j represent all the atoms of the oligomer. The Coulomb interactions are parameterized according to the Ohno relationship [23],

$$V_{i,j} = U/\kappa_{i,j}(1 + 0.6117R^2_{i,j})^{1/2} \ , \tag{4}$$

where, $\kappa_{i,j,M,N}$ depicts the dielectric constant of the system which can simulate the effects of screening, U is the on-site repulsion term, and $R_{i,j}$ is the distance in Å between the ith carbon and the the jth carbon. The values of U and $\kappa_{i,j,M,N}$ are unknown quantities and, at present, it is not clear as to what range of values of these parameters are suitable for PDPA's. In our earliear studies of linear optics of these materials we tried two parameter sets: (a) "standard parameters" with $U = 11.13$ eV and $\kappa_{i,j} = 1.0$, and (b) "screened parameters" with $U = 8.0$ eV and $\kappa_{i,i,M,M} = 1.0$, and $\kappa_{i,j,M,N} = 2.0$, otherwise[17,18,19]. Using the screened parameters, Chandross and Mazumdar[24] obtained better agreement with experiments on excitation energies of PPV oligomers, as compared to the standard parameters. Recently, we performed a large-scale correlated study of singlet and triplet excited states in oligo-PPV's and observed a similar trend[8]. As far as the hopping matrix elements are concerned, for correlated calculations we used the same values for these parameters as in the independent electron calculations except for the value of Δt which was taken to be 0.168 eV.

The starting point of the correlated calculations for various oligomers were the restricted Hartree-Fock (HF) calculations, using the P-P-P Hamiltonian. The many-body effects beyond HF were computed using different levels of the configuration interaction (CI) method, namely, singles-CI (SCI), quadruples-CI (QCI), and the multi-reference singles-doubles CI (MRSDCI). Since the number of electrons in oligo-PDPA's is quite large despite the P-P-P approximation owing to the large unit cell (fourteen electrons/cell), except for the SCI calculations, it is not possible to include all the orbitals in the many-body calculations. Therefore, one has to reduce the number of degrees of freedom by removing some orbitals from the many-body calculations. In order to achieve that, for each oligomer we first decided as to which occupied and the virtual orbitals will be active in the many-body calculations based upon: (a) their single-particle HF energies with respect to the location of the Fermi level, and (b) Mulliken populations of various orbitals with respect to the chain/phenylene-based atoms. Because of the particle-hole symmetry in the problem, the numbers of active occupied and virtual orbitals were taken to be identical to each other, with the occupied and virtual orbitals being particle-hole symmetric. The remaining occupied orbitals were removed from the many-body calculations by the act of "freezing", i.e., by summing up their interactions with the active electrons, and adding this effective potential to the one-electron part of the total Hamiltonian. The inactive virtual orbitals were simply deleted from the list of orbitals. When we present the CI results on various oligo-PDPA's, we will also identify the list of active orbitals. During the CI calculations, full use of the spin and the point group (C_i for PDPA's) symmetries was made. From the CI calculations, we obtain the eigenfunctions and eigenvalues corresponding to the correlated ground and excited states of various oligomers. Using the many-body wave functions, we compute the matrix elements of the dipole operator amongst various states. Finally, these

quantities are fed in to the sum-over-states formulas of Orr and Ward, [26] to obtain the correlated values of the TPA susceptibility $\chi^{(3)}(-\omega;\omega,-\omega,\omega)$. More details about the procedural aspects of various CI approaches used by us can be found in our earlier works[8,18,19,25].

3 Results and Discussion

In this section we present our results on the TPA susceptibilities of oligo-PDPA's, computed using various approaches. Where applicable, we also compare our results for the oligo-PDPA's to the corresponding results on polyenes of the same conjugation length.

3.1 Independent-Electron Theory

In this section we briefly present and discuss the TPA spectra of oligo-PDPA's computed using the independent-particle Hückel model. First we present the results on the longitudinal component of the susceptibility, followed by those on the transverse component.

3.1.1 Longitudinal Component

The longitudinal component of the two-photon absorption spectrum, $\chi^{(3)}_{xxxx}(-\omega;\omega,-\omega,\omega)$, for oligo-PDPA's describes the longitudinal nonlinear optical response of the material to the radiation polarized along the conjugation direction (x-axis). [21] It is represented by the imaginary part of $\chi^{(3)}_{xxxx}(-\omega;\omega,-\omega,\omega)$, calculated values of which for PDPA-50 are presented in Fig.2. For the sake of comparison, the same figure also presents the longitudinal TPA spectrum of fifty unit cell polyene. Although the plots of the TPA spectra of the two materials appear qualitatively similar, however, there are significant quantitative differences between the two. It is obvious from Fig. 2 that: (a) The magnitude of the resonant nonlinear response in PDPA is significantly enhanced as compared to the *trans*-polyacetylene, and (b) all the resonant features of the two-photon spectrum of the PDPA are significantly redshifted as compared to *trans*-polyacetylene. Although, in Fig.2 the TPA spectra of relatively larger oligomers of the two substances are compared, the same trend is obvious even for small oligomer such as PDPA-5, when compared to a polyene of the same size. Thus Hückel model calculations on both small and large oligomers suggest that the resonant parts of the longitudinal component of the TPA of PDPA's are significantly more intense, and redshifted, compared to *trans*-polyacetylene. This point can be further understood by referring to

Fig. 3, in which the energy levels of a ten unit polyene and PDPA-10 are presented side by side. From the figure it is obvious that all comparable energy gaps, including the optical gap, are narrowed in PDPA, as compared to the corresponding polyene.

Next we study the many-particle states which are visible in the TPA spectrum of various oligomers of PDPA. For the purpose, we denote the highest occupied molecular orbital (HOMO) as H, and the lowest unoccupied molecular orbital (LUMO) as L. For PDPA-10, the most intense peak corresponds to the $2A_g$ state of the oligomer obtained by $|H \rightarrow L+1\rangle$ and $|H-1 \rightarrow L\rangle$ singlet excitations (see Fig. 3 for the energy levels). However, as the size of the oligomer increases, the $2A_g$ state ceases to be the most intense peak. For example, in the TPA spectrum of PDPA-30, the $3A_g$ state corresponding to the $|H \rightarrow L+3\rangle$ and $|H-3 \rightarrow L\rangle$ excitations is the most intense peak. This trend continues with the increasing size of the oligomer, and we speculate that the longitudinal TPA spectrum of an infinite PDPA would be a broad resonance, with several A_g-type states contributing to the intensity, in perfect qualitative agreement with the TPA spectrum of infinite *trans*-polyacetylene. [2] The other noticeable aspect of these A_g-type states is that they all originate from the excitations among the orbitals close to the Fermi level, which have polyene-like character, with large Mulliken population of sites located on the backbone. Thus, we conclude that, as far as the independent-electron theory is concerned, the longitudinal TPA spectrum of PDPA is qualitatively similar to that of *trans*-polyecetylene.

3.1.2 Transverse Component

Imaginary part of the susceptibility component $\chi^{(3)}_{yyyy}(-\omega;\omega,-\omega,\omega)$ describes the lowest-order nonlinear optical absorption of the transversely polarized radiation in oligo-PDPA's. It is this component of the susceptibility which distinguishes the nonlinear response of PDPA from that of *trans*-polyacetylene. Clearly, due to minimal extension in the transverse direction, *trans*-polyacetylene will have negligible values of this component. In Fig. 4 we plot on the same scale, both the longitudinal, and the transverse, components of the TPA susceptibility for PDPA-50 computed using the Hückel model.

From Fig. 4, it is clear that: (a) the resonant intensities of the transverse component of the susceptibility within the Hückel model are comparable to that of the longitudinal ones, (b) the excited states contributing to the transverse component are much higher in energy as compared to the ones contributing to the longitudinal component. Moreover, the transverse component displays very weak size dependence as far as the location of the main peak is concerned which, for all the oligomers studied, is roughly close to 1.7 eV. The weak size dependence of the resonant energy suggests that the excited states in question

A. Shukla : Fig 2

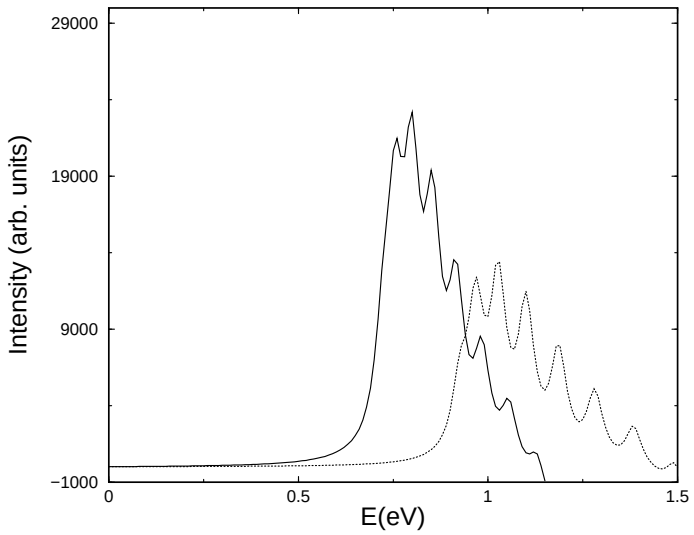

Figure 2. Comparison of the imaginary part of $\chi^{(3)}_{xxxx}(-\omega;\omega,-\omega,\omega)$ of PDPA (solid line) and *trans*-polyacetylene (dotted line) oligomers containing fifty unit cells, computed using the Hückel model. With our choice of hopping parameters (see text) optical gap of PDPA-50 was computed to be 1.42 eV, while that of the *trans*-polyacetylene oligomer was 1.82 eV. A linewidth of 0.05 eV was assumed for all energy levels.

must involve phenyl derived single-electron levels, because with the increasing conjugation length of the oligomer, its size in the transverse direction remains unchanged. Next we investigate the energy levels involved in the transverse TPA susceptibilities of PDPA's.

Since the number of one-electron levels proliferates tremendously with the increasing conjugation length due to band formation, it is fruitful first to investigate smaller oligomers such as PDPA-10. In PDPA-10, the main peak occurs at 1.71 eV which corresponds to an A_g type state obtained from the ground state by single-excitations $H \rightarrow L+39$ and $H-39 \rightarrow L$. To investigate the nature of the orbital corresponding to the $L+39$-th one-electron state, we calculated the contribution of the charge density centered on the backbone carbon atoms, to its total normalization. The contribution was computed to be 0.05 which indicates that the orbital in question is predominantly centered on the side phenyl rings. Further investigation of the orbital coefficient reveals that the orbitals in question, are derived from the phenyl-based delocalized (d^*) virtual orbitals, with no contribution from the localized orbitals (l^*-type) of the phenyl rings. Similarly, owing to the particle-hole symmetry, $H-39$-th orbital is derived from the d-type occupied orbitals of the phenyl rings. The energy levels corresponding to these orbitals are presented in Fig. 3.

Next we examine the case of PDPA-50, for which the highest peak is located at

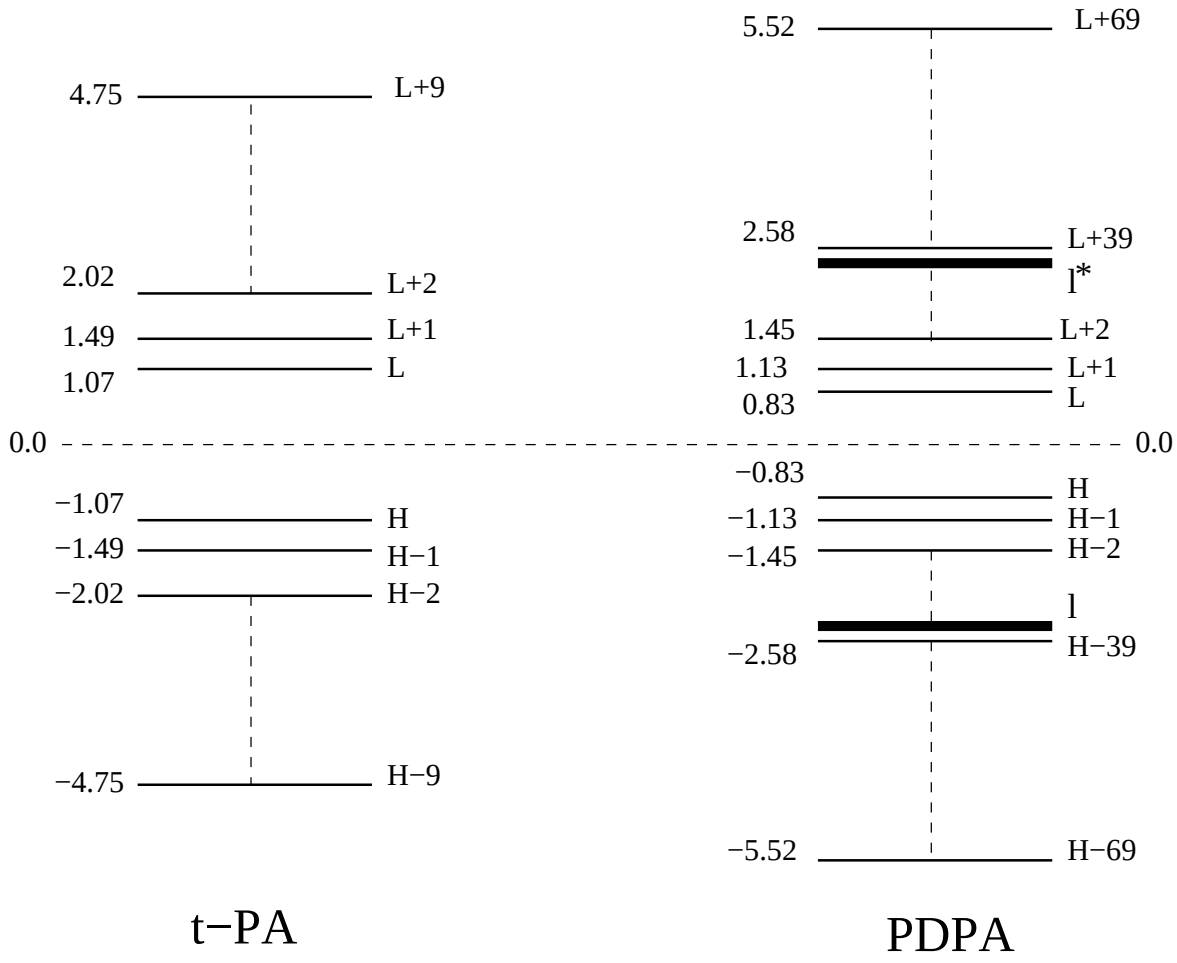

A. Shukla: Fig 3

Figure 3. Important single particle energy levels of ten unit oligomers of *trans*-polyacetylene (labeled t-PA) and PDPA computed using the Hückel model. Energy levels are drawn to the scale, with their values (in eV) indicated next to them. Chemical potential is indicated as the dotted line through the center, and is assumed to be 0.0 eV. For the chosen hopping parameters (see text), the optical gap in PDPA oligomer is 1.66 eV as compared to 2.14 eV in the t-PA oligomer. As per the notation explained in the text, H/L indicate HOMO/LUMO orbitals. The thick lines labaled l/l^*denote the localized orbitals of phenyl rings, all of which are located at -2.4/2.4 eV. In addition to the optical gap, narrowing of other energy gaps in PDPA, as compared to t-PA, is obvious.

1.72 eV. Here we find that most of the states in this energy region correspond to single-excitations $H-5 \rightarrow L+153+i$ (and its particle-hole reversed counterpart) with $\{i=0,\ldots,8\}$. Again a charge density analysis of these levels reveals that while the levels $H-5$ (and $L+5$) have chain atom contribution of ≈ 0.72, while the levels $L+153+i$ (and $H-153-i$) have chain atom

A. Shukla: Fig. 4

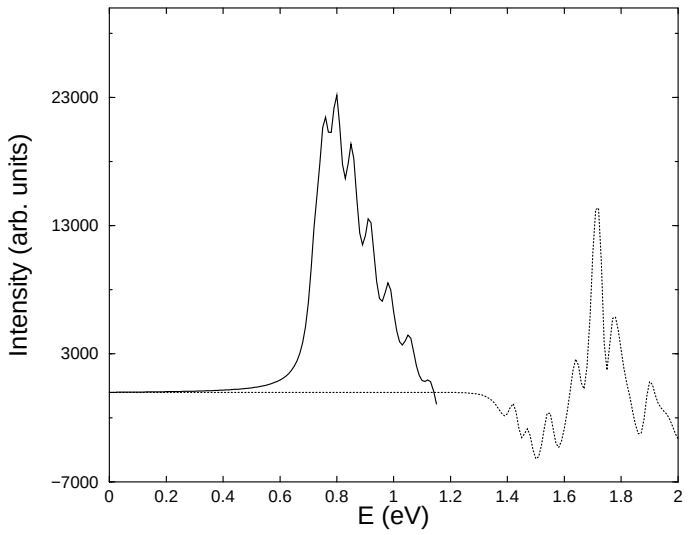

Figure 4. Comparison of the longitudinal (solid lines) and the transverse (dotted lines) components of the TPA susceptibilities for a PDPA oligomer containing fifty unit cells, computed using the Hückel model. Linewidth of 0.05 eV was assumed for all energy levels.

contribution to the total normalization ≈ 0.01. Thus it is clear that $H-5$ ($L+5$) orbital constitutes top of the valence band (bottom of the conduction band) composed of the chain levels, while the orbital coefficients reveal that the levels $H-153-i$ ($L+153+i$) are part of the occupied (unoccupied) bands composed predominantly of the phenyl-based d (d^*) levels. Thus it is clear that the transverse TPA susceptibility of the system owes its origins to phenyl-based levels. This is an important point which also helps us perform effective correlated calculations of this component, presented next.

3.2 Correlated-Electron Theory

Based upon correlated-electron calculations performed on polyenes, a simplified picture of their nonlinear optical properties—referred to us "essential-states picture"—has emerged[3,4]. According to this picture, most of the nonlinear optical properties of polyenes can be understood based upon the excited states $1B_u$ (the lowest one-photon state), mA_g (a state with strong dipole coupling to $1B_u$), and nB_u (a state with strong dipole coupling to mA_g). Although, the state $2A_g$ (a two-photon state lower in energy than $1B_u$ in polyenes) also has a large dipole coupling to the $1B_u$ state, its contribution to nonlinear susceptibilities becomes very small due to some curious cancellation effects resulting from the many-body nature of these states[3,4]. For the particular case of TPA susceptibility, in polyenes one observes a weak peak corresponding to the $2A_g$ state, while the most intense peak is derived from the mA_g state

arising from the excitation channel $1A_g \rightarrow 1B_u \rightarrow mA_g \rightarrow 1B_u \rightarrow 1A_g$[3,4]. Because of the structural similaritiy of PDPA to *trans*-polyacetylene, while presenting our results we will analyze them from the standpoint of the essential states mechanism. Moreover, since the transverse nonlinear spectrum of these materials is completely novel as compared to the polyenes, one wonders whether an essential states mechanism also holds for this component as well.

First, however, we briefly elucidate the role played by the choice of Coulomb parameters in the P-P-P model, because, as mentioned earlier correct parameters are still unknown for PDPA's, thereby making the choice of these parameters very important.

3.2.1 Role of Coulomb parameters

In the present work, we have performed the calculations using both the standard Ohno parameters, as well as the screened parameters of Chandross and Mazumdar[24] to describe the P-P-P Hamiltonian. However, based upon our earlier calculations dealing with the optical properties of PDPA[17,18,19], and PPV[8,25], the screened-parameter-based calculations generally yield much better agreement with experiments than the ones based upon the standard parameters. The standard-parameter-based calculations for such systems generally yield energy gaps which are larger than the experimental ones. In Fig.5 we compare the longitudinal components of the TPA spectra ($\chi^{(3)}_{xxxx}(-\omega;\omega,-\omega,\omega)$) for PDPA-5 computed both with the standard and the screened parameters, using the SCI approach. It is clear from the figure that qualitatively speaking both the spectra are similar. However, from a quantitative viewpoint: (a) the intensities are significantly larger as computed with the screened parameters, (b) and more importantly the resonant features of the screened spectrum are substantially red-shifted as compared to the standard spectrum.

Since the smaller energy gaps obtained with the screened parameters in our earlier works were found to be in much better agreement with the experiments, we will present our main results based upon screened-parameter-based calculations. However, when we compare the PDPA nonlinear optical spectra with those of polyenes, we will use the standard parameters because screened parameters are not valid for polyenes.

3.2.2 Longitudinal Component

Imaginary parts of $\chi^{(3)}_{xxxx}(-\omega;\omega,-\omega,\omega)$, calculated with screened parameters and the SCI and QCI approaches for PDPA-5 and PDPA-10 are presented in Fig.6.

Energies and many-particle wave-functions of various A_g-type excited states

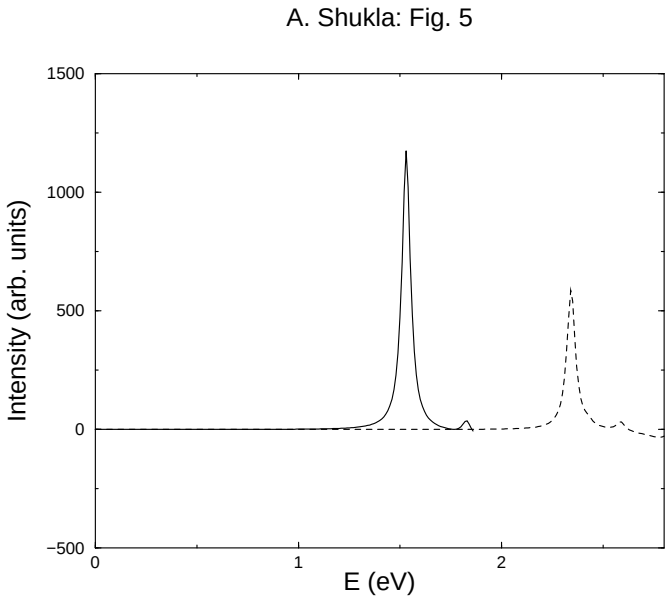

Figure 5. Comparison of imaginary parts of $\chi^{(3)}_{xxxx}(-\omega;\omega,-\omega,\omega)$ spectra of PDPA-5 computed with screened parameters (solid line) and standard parameters (broken line). A linewidth of 0.05 eV was assumed and the SCI method was used to compute the excited states.

contributing to peaks in different spectra are summarized in table 1 for PDPA-5 and in table 2 for PDPA-10.

First, we will discuss the results obtained using the SCI approach, presented in Figs. 6(a), and 6(c). Although, the SCI approach does not include the electron correlation effects to a high order, it does include them in a more balanced way for the ground and the excited states as compared to the singles-doubles-CI (SDCI) approach. Therefore, it provides a feel for the influence of electron correlation effects on various properties. Moreover, since it is computationally not very expensive, it allows us to include all the orbitals in the calculations which is certainly not possible for large systems such as oligo-PDPA's if some more extensive approach such as MRSDCI/QCI were used. An inspection of the spectra reveals the following general features: (i) The susceptibilities of both the oligomers have only one intense peak while, with the increasing sizes of oligomers, as expected, the peak is redshifted and becomes much more intense.

Next we examine the SCI many-particle wave functions of the states contributing to the peaks in the longitudinal TPA spectra. For PDPA-5 (Fig. 6(a)), the peak in the TPA spectrum corresponds to the $2A_g$ state located at 3.06 eV whose SCI wave function gets its main contributions from the singly excited configurations $|H \rightarrow L+1\rangle$ and $|H-1 \rightarrow L\rangle$ with coefficients 0.69 denoted in short as $|H \rightarrow L+1\rangle + c.c.$ (0.69) in table 1[27]. Many other singly-excited configurations make smaller contributions to the total wave function. For the

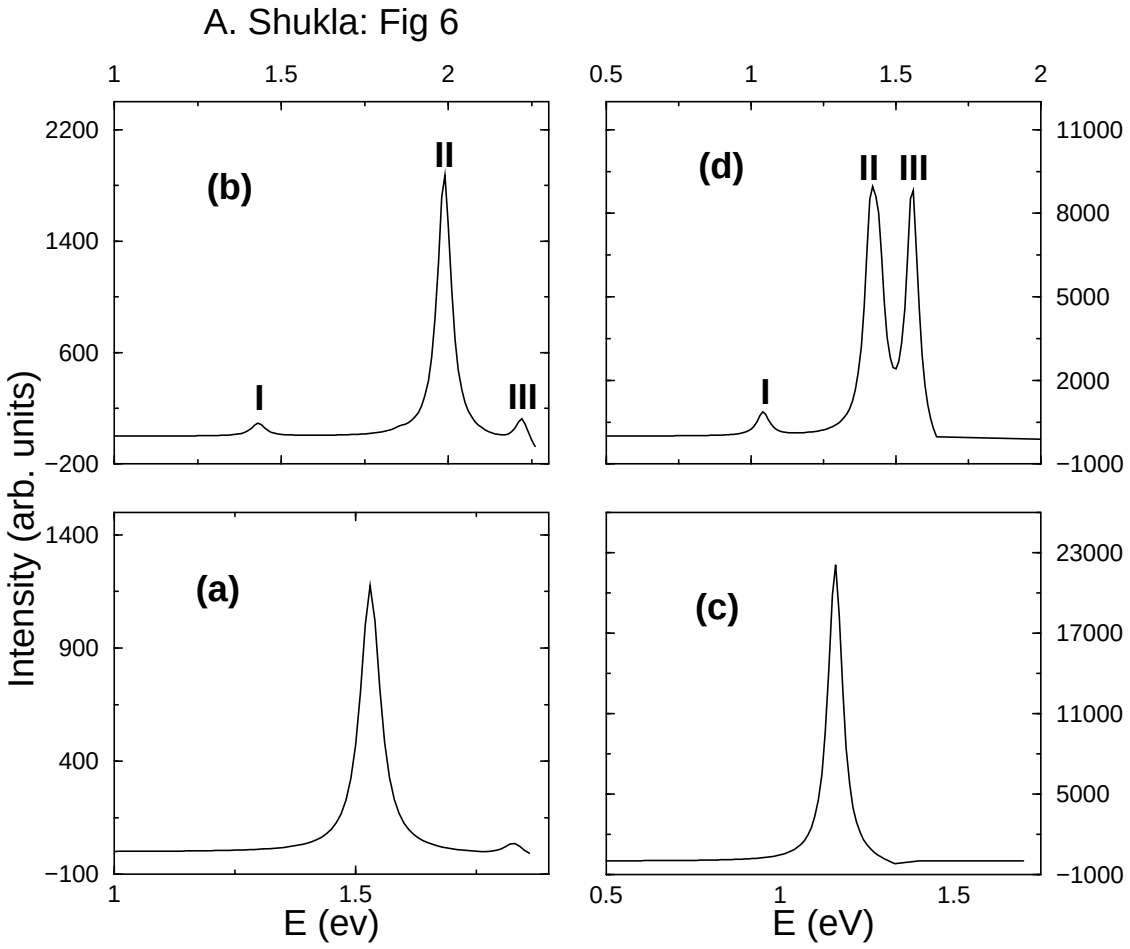

Figure 6. Imaginary parts of the longitudinal two-photon absorption spectra ($\chi^{(3)}_{xxxx}(-\omega;\omega,-\omega,\omega)$) of oligo-PDPA's calculated using various CI approaches and the screened parameters: (a) PDPA-5 (SCI), (b) PDPA-5 (QCI), (c) PDPA-10 (SCI), and (d) PDPA-10 (QCI). A common linewidth of 0.05 eV was assumed for all the levels.

case of PDPA-10 (Fig. 6(c)), as is clear from table 2, the peak again corresponds to the $2A_g$ state, located at a lower energy, has a many-particle wave function qualtitatively identical to that for PDPA-5. Since at the SCI level, the many-particle wave function is missing two-particle excitations, therefore, the $2A_g$ state actually corresponds to the mA_g state obtained at a higher energy in more sophisticated calculations such as the QCI[28]. Clearly, the picture emerging from the SCI calculations is that it is the A_g-type excited states resulting from single-particle excitations among the orbitals close to the Fermi level which contribute to the main intensity in the longitudinal TPA spectrum. Clearly, this picture is in very good agreement with the Hückel-model-based results reported in the previous section.

Therefore, now it is of interest to explore as to how high-order correlation treatments such as the QCI approach influence these properties. However, given the large number of electrons in these systems, QCI method is not feasible for

them if all the orbitals of the system are retained in the calculations. Since the longitudinal nonlinear optical properties are determined by low-lying excited states of the system, in the limited CI calculations we decided to include the orbitals closest to the Fermi level. Therefore, for PDPA-n we included n occupied, and n virtual orbitals closest to the Fermi level in the QCI calculations. Remaining occupied orbitals were frozen and virtual orbitals were deleted as explained in section 2. Thus, the computational effort associated with the QCI calculations on PDPA-n is same as that needed for a polyene with n double bonds. Although for PDPA-10, it leads to Hilbert space dimensions in excess of one million, however, using the methodology reported in our earlier works[8,18], we were able to obtain low-lying excited states of such systems.

In Figs. 6(b) and 6(d) we present the longitudinal TPA susceptibilities of PDPA-5 and PDPA-10 computed using the QCI approach, and utilizing the screened-parameters in the P-P-P Hamiltonian. It is clear from the figures that that the longitudinal TPA spectra at the QCI/screened level exhibit three peaks (labeled I, II, and III) while the corresponding SCI spectrum presented earlier exhibited only one peak. Peak I is a weak feature which corresponds to the $2A_g$ states of both the oligomers. Due to the better treatment of electron correlation effects, one obtains a $2A_g$ state which is distinct from the mA_g state both in excitation energy, and contribution to the TPA spectrum. The $2A_g$ state, in complete analogy with the situation in polyenes, is mainly composed of low-lying single and double excitations and makes a negligible contribution to the longitudinal TPA spectra of oligo-PDPA's. This aspect of electron correlation effects has been observed over the years in the calculations on polyenes[4], and recently on PPP and PPV polymers as well[25], where the contribution of the $2A_g$ state to the TPA spectrum diminishes once sophisticated many-body techniques are employed to describe the excited states.

Feature II of PDPA-5 is due to the $4A_g$ state of the oligomer, while in PDPA-10 it derives its intensity from two nearly degenerate states $3A_g$ and $4A_g$. Since this feature corresponds to the most intense peak in the spectrum, based on that that crieterion alone, one is tempted to label it as the mA_g state of the corresponding oligomer. When we compare the many-particle state of mA_g to that of $2A_g$, we observe that the same configurations ($|H \rightarrow L; H \rightarrow L\rangle$ and $|H-1 \rightarrow L+2\rangle + c.c$) make the most important contributions to both the states, a feature again in common with the trend seen in polyenes[4], and PPP and PPV[25]. Finally, when we examine the longitudinal dipole couplings of these states with the $1B_u$ state, we observe that it is much higher for the $mA_g - 1B_u$ coupling as compared to the $2A_g - 1B_u$ coupling, clearly explaining the relative intensity pattern of the longitudinal TPA spectra of oligo-PDPA's. Based upon this we conclude that the feature II of the spectrum indeed corresponds to the mA_g states of the respective oligomers.

Finally, feature III in PDPA-5 is a rather weak feature while, in PDPA-10,

Table 1
Nature of A_g type states contributing to the longitudinal TPA spectrum of PDPA-5 as obtained in various CI calculations. Under the heading wave function, we list the most important configurations contributing to the many-body wave function of the state concerned, along with their coefficients, consitent with our convention[27].

Calculation	Feature	State	Energy (eV)	Wave Function
SCI	I	$2A_g(mA_g)$	3.06	$\|H \rightarrow L+1\rangle + c.c$ (0.69)
QCI	I	$2A_g$	2.86	$\|H \rightarrow L+1\rangle + c.c.$ (0.57)
				$\|H \rightarrow L; H \rightarrow L\rangle$(0.48)
QCI	II	$4A_g(mA_g)$	3.98	$\|H \rightarrow L+1\rangle + c.c.$(0.37)
				$\|H \rightarrow L; H \rightarrow L\rangle$(0.74)
QCI	III	$5A_g$	4.44	$\|H-1 \rightarrow L+2\rangle + c.c.$(0.55)
				$\|H-2 \rightarrow L; H \rightarrow L\rangle + c.c.$(0.24)
				$\|H-1 \rightarrow L; H \rightarrow L+1\rangle$(0.23)

it is a very intense peak. In both the oligomers this feature is due to the $5A_g$ states whose many-particle wave function is listed in tables 1 and 2 are qualitatively similar. In both the oligomers this state is a linear combination of higher-energy singly- and doubly-excited configurations. However, the fact that, contrary to PDPA-5, in PDPA-10 this state has a strong dipole coupling to the $1B_u$ state clearly points to the band formation and suggests the possibility that in longer oligomers this feature will merge with feature II leading to a single mA_g band.

Next, we compare the longitudinal component of the TPA spectra of PDPA with that of *trans*-polyacetylene for calculations performed at the QCI level, using the standard parameters for the P-P-P Hamiltonian. The imaginary parts of longitudinal TPA spectra of ten unit oligomers of PDPA and *trans*-polyacetylene are presented in Fig. 7. The spectrum of *trans*-polyacetylene oligomer has only one significant peak corresponding to the mA_g state while that of PDPA-10 has again three visible features to which states $2A_g$, $4A_g$, and $6A_g$ contribute. Although, the many-body wave functions of these states are similar to the corresponding states obtained with the screened parameters (see discussion above), however, unlike the case for screened parameters, only one of the three peaks ($6A_g$) in the PDPA-10 spectrum is intense which clearly corresponds to the mA_g, state of the oligomer. This is in excellent qualitative agreement with the TPA spectrum of *trans*-polyacetylene which also shows only one intense peak corresponding to its mA_g state. As far as the quantitative comparisons between the two are concerned, it is clear that the peak intensities in PDPA are significantly larger as compared to the *trans*-polyacetylene, and all the peaks in the TPA spectrum of the PDPA are substantially redshifted as compared to *trans*-polyacetylene. It is noteworthy that we obtain this result

Table 2
Nature of A_g-type states contributing to the longitudinal TPA spectrum of PDPA-10 in various CI calculations. Rest of the information is same as given in the caption of table 1.

Calculation	Feature	State	Energy (eV)	Wave Function
SCI	I	$2A_g(mA_g)$	2.32	$\|H \rightarrow L+1\rangle + c.c$ (0.68)
QCI	I	$2A_g$	2.08	$\|H \rightarrow L+1\rangle + c.c.$ (0.49)
				$\|H \rightarrow L; H \rightarrow L\rangle$(0.50)
QCI	II	$3A_g(mA_g)$	2.82	$\|H \rightarrow L+1\rangle + c.c.$(0.68)
		$4A_g(mA_g)$	2.88	$\|H \rightarrow L; H \rightarrow L\rangle$(0.37)
QCI	III	$5A_g(mA_g)$	3.11	$\|H \rightarrow L+3\rangle + c.c.$(0.42)
				$\|H \rightarrow L+1\rangle + c.c.$(0.27)
				$\|H \rightarrow L; H \rightarrow L\rangle$(0.33)
				$\|H-1 \rightarrow L; H \rightarrow L+1\rangle$(0.31)
				$\|H \rightarrow L+1; H \rightarrow L+3\rangle + c.c.$(0.27)

A. Shukla: Fig 7

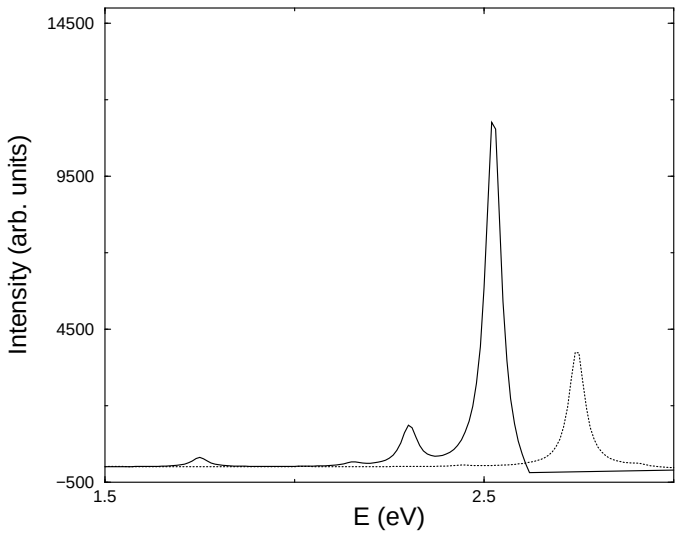

Figure 7. Comparison of the imaginary parts of $\chi^{(3)}_{xxxx}(-\omega;\omega,-\omega,\omega))$ computed with the QCI method and the standard parameters for ten repeat unit oligomers of: (a) PDPA (solid lines) and (b) *trans*-polyacetylene (dotted lines). A linewidth of 0.05 eV was assumed for all the levels.

despite the fact that from the correlated calculations on PDPA-10 we have deleted all the orbitals except the ten most "chain-like" orbitals. This clearly indicates that the presence of side phenyl rings changes the nature of even the chain-like levels in such a way that they lead to an enhanced nonlinear

response. The results of these correlated calculations also confirm the results of our Hückel model calculations presented in the previous section where we arrived at the same conclusions regarding the longitudinal TPA spectrum of PDPA vis-a-vis *trans*-polyacetylene.

Thus the main conclusion of the present section is that as far as the longitudinal TPA spectrum of PDPA is conerned, our calculations suggest that, similar to the case of *trans*-polyacetylene, it will have one intense peak corresponding to the mA_g state of the system.

3.2.3 Transverse Component

Performing accurate correlated calculations of $\chi^{(3)}_{yyyy}(-\omega;\omega,-\omega,\omega)$ for oligo-PDPA's is an extremely difficult task. The reason behind this is that the many-body A_g-type states which contribute to the peaks in this component of the susceptibility are very high in energy, and thus are more difficult to compute by many-body methods as compared to the low-lying excited states contributing to the longitudinal spectra. The very high excitation energies of these states are due to the fact that these A_g-type states are predominantly composed of excited configurations involving high-energy delocalized orbitals originating from the side benzene rings. Therefore, it is clear that the SCI approach, at best, may provide a qualitative picture of transverse nonlinear optical properties of PDPA's, and, that too, for smaller oligomers. For larger oligomers, results obtained with the SCI approach will not be very reliable. However, during our independent-electron study, we concluded that transverse susceptibilities exhibit rapid saturation with the conjugation length. Therefore, we restrict our study of the transverse components of the nonlinear susceptibilities to PDPA-5. We perform calculations using the screened parameters both at the SCI, as well as at the MRSDCI level. The SCI calculations were performed using all the orbitals of the oligomer while, the more rigorous MRSDCI calculations were performed using thirty orbitals in all, of which fifteen were occupied orbitals, and the remaining fifteen were the virtual ones. Rest of the occupied orbitals were frozen. Of the thirty orbitals, ten were the orbitals closest to the Fermi level which were also used in the QCI calculations. Remaining twenty orbitals were the d/d^*-type phenylene-ring-based orbitals closest to the Fermi level. In the MRSDCI calculations, no l/l^*-type phenylene orbitals were used because they do not make any significant contribution to the transverse nonlinear spectra either in the Hückel model calculations, or in the SCI calculations. In the MRSDCI calculations, we used 25 reference configurations for the A_g-type states, and 24 for the B_u-type states leading to CI matrices of dimensions close to half-a-million both for the A_g and B_u manifolds.

The transverse TPA spectra of PDPA-5 computed by us are presented in Fig.

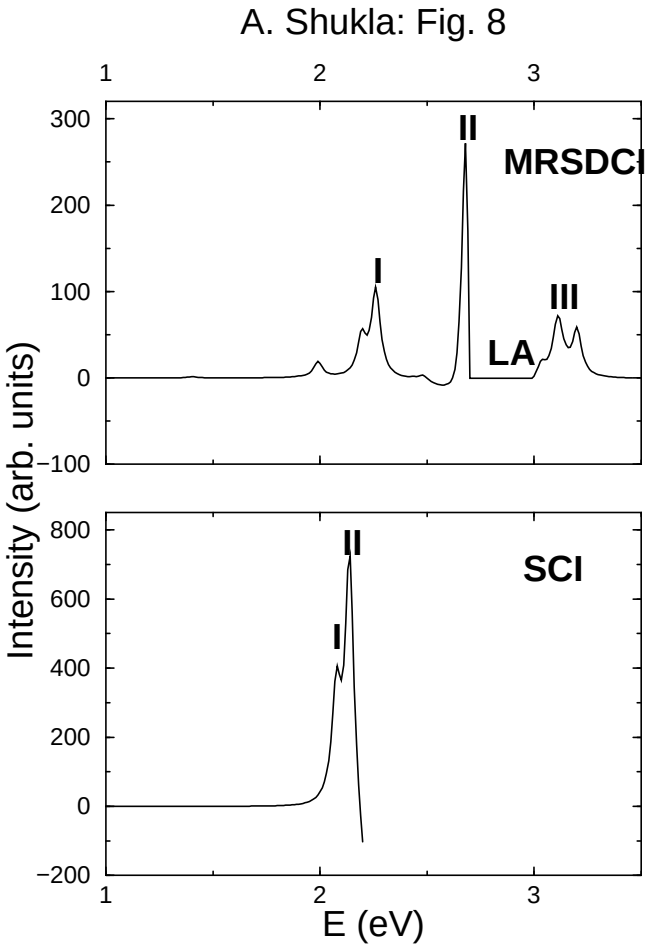

Figure 8. Imaginary part of $\chi^{(3)}_{yyyy}(-\omega;\omega,-\omega,\omega))$ of PDPA-5 computed using the screened parameters and: (a) SCI method (bottom), and (b) MRSDCI method (top) . A linewidth of 0.05 eV was assumed for all the levels.

8.

The many-particle wave functions of various states contributing to these spectra are presented in table 3. The SCI spectrum exhibits only one intense peak (feature II) accompanied by a shoulder (feature I). Upon examining the many-body states contributing to these peaks in table 3, we conclude that both these features are due to A_g-type states whose wave function consists of single excitations involving L/H orbitals, and the high-energy d/d^* class of orbitals $(H-17, H-19, L+17, L+19)$ localized on the benzene rings. Thus, nature of states contributing to the transverse TPA spectrum at the SCI level is the same as that obtained at the independent particle level.

Upon examining the MRSDCI spectrum of Fig. 8, we see a significant redistribution of intensity over several peaks, as compared to the SCI spectrum. As a result, the intensity of the highest peak in the MRSDCI spectrum is much smaller as compared to the highest one in the SCI spectrum. Next, we discuss the excited states contributing to the three main features of the spectrum

Table 3
A_g-type states contributing to the transverse TPA spectrum of PDPA-5 computed by various CI methods. Rest of the information is same as given in the caption of table 1.

Calculation	Feature	State	Energy (eV)	Wave Function
SCI	I	$9A_g$	4.15	$\|H \rightarrow L+17\rangle + c.c\,(0.40)$
				$\|H \rightarrow L+19\rangle + c.c\,(0.33)$
SCI	II	$11A_g$	4.28	$\|H \rightarrow L+17\rangle + c.c\,(0.38)$
				$\|H \rightarrow L+19\rangle + c.c\,(0.54)$
MRSDCI	I	$6A_g$	4.52	$\|H \rightarrow L+17\rangle + c.c\,(0.27)$
				$\|H \rightarrow L+19\rangle + c.c\,(0.38)$
				$\|H-2 \rightarrow L+1\rangle + c.c\,(0.30)$
MRSDCI	II	$12A_g$	5.36	$\|H-1 \rightarrow L+2\rangle + c.c.(0.34)$
				$\|H-1 \rightarrow L+1; H \rightarrow L\rangle(0.39)$
				$\|H-1 \rightarrow L; H-1 \rightarrow L\rangle + c.c.(0.35)$
MRSDCI	III	$17A_g$	6.25	$\|H \rightarrow L+19\rangle + c.c.(0.35)$
				$\|H-1 \rightarrow L+1; H \rightarrow L\rangle(0.39)$

labeled I, II, and III. The region labeled LA corresponds to the region of the spectrum where y-polarized linear absorption dominates and thus the actual TPA intensity there has large negative values. For the sake of convenience, we have set the intensity in that region to zero. Feature I, which is mainly due to the $6A_g$ state, is composed primarily of single excitations involving L/H and the phenyl-based d/d^* orbitals, and has a large coupling to the $1B_u$ state via y-component of the dipole operator. Although peak I of the MRSDCI spectrum is much weaker in intensity as compared to its SCI counterpart, the nature of the many-body state contributing to the peak in the MRSDCI spectrum is very similar to the ones contributing to features I and II of the SCI spectrum.

Feature II is the most intense peak of the spectrum and it is due to a high energy state $12A_g$ located at 5.36 eV which also has a significant y-dipole coupling to the $1B_u$ state. However, $12A_g$ state is qualitatively distinct from the $6A_g$ state in that it exhibits strong mixing of singly- and doubly-excited configurations involving low-lying orbitals, with no significant contribution from the configurations involving the phenyl-based d/d^* orbitals. This result, which is qualitatively new when compared to the Hückel model or the SCI results, is, clearly, an example of the superior treatment of electron correlation effects by the MRSDCI approach, because the double excitations are completely absent from the SCI wave functions. Finally, feature III, which is also the last feature of the MRSDCI spectrum, is mainly due the $17A_g$ state whose many-particle

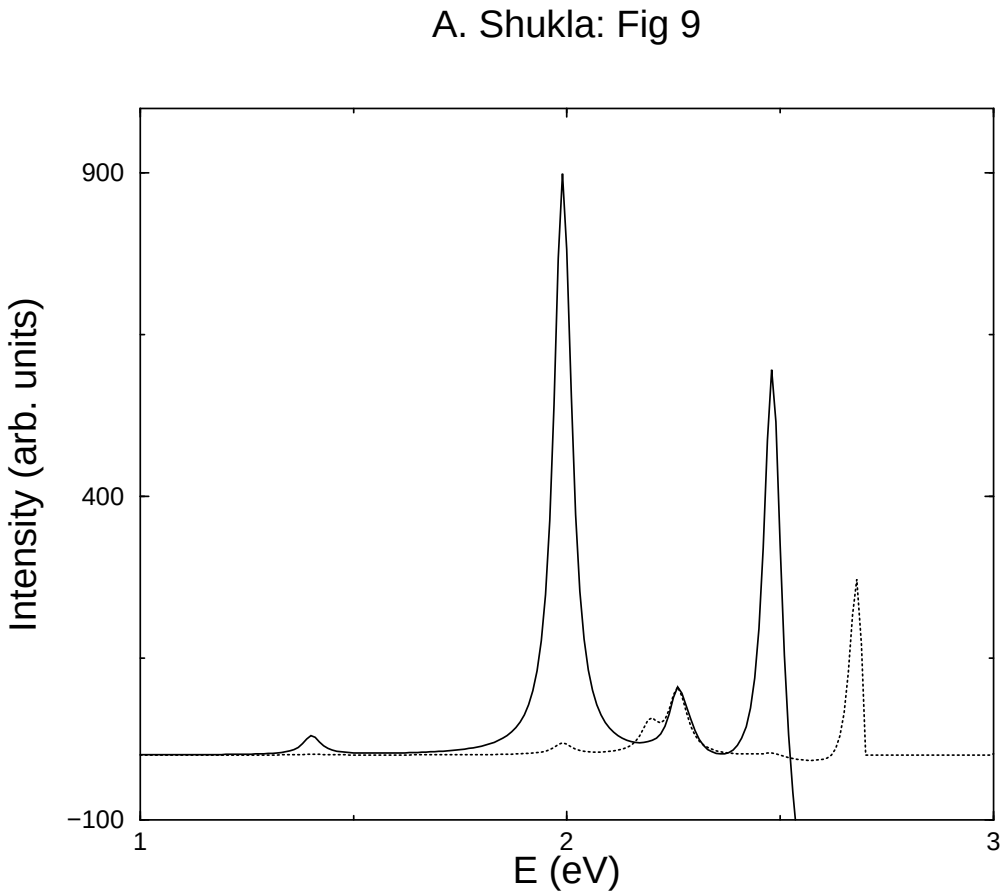

Figure 9. Comparison of longitudinal (solid lines) and the transverse (dotted lines) two photon absorption spectra of PDPA-5 computed using the screened parameters and the MRSDCI method. A linewidth of 0.05 eV was assumed for all the levels.

wave function is also different from those of previous states in that it is composed of double excitations involving low-lying orbitals, and single excitations involving H/L and phenyl-based d/d^* orbitals.

In Fig. 9 we compare the MRSDCI transverse TPA spectrum of PDPA-5 with its longitudinal one, and find that although transverse TPA resonant intensities are considerable, but they are weaker than their longitudinal counterparts. Clearly, the height of the most intense peak in the transverse spectrum is about one-fourth the height of the strongest peak of the longitudinal spectrum. We speculate that the reason behind this result is that electron correlation effects redistribute the intensity in the transverse spectrum over several peaks, making the resonant response weaker. Therefore, it will be of considerable interest to perform correlated calculations on longer oligomers to check whether aforesaid results hold true in the bulk limit as well.

4 Conclusions and Future Directions

Our aim behind undertaking the present theoretical study of the nonlinear optical properties of the novel polymer PDPA was, not only to calculate its TPA spectra, but also to understand them in a way similar to what has been possible for simpler polymers such as *trans*-polyacetylene[3,4], PPP, and PPV[7,25], i.e. in terms of an essential state mechanism involving a small number of excited states. For PDPA's, whose structure has ingredients in common with both the chain-like, as well as the phenyl-based polymers, our calculations suggest that their longitudinal nonlinear optical properties can certainly be understood in terms of an essential state mechanism, with the mA_g state being the dominant feature in the spectrum. Thus, so far as the longitudinal TPA spectrum of oligo-PDPA's is concerned, the system behaves as though it were a polyene with different hopping and electron-repulsion parameters so as to account for its lower optical gaps, and enhanced resonant response.

As far as the tranverse spectrum is concerned, our calculations performed on PDPA-5 suggest that there are three main features contributing to the TPA spectrum, if sophisticated correlated calculations are performed. Therfore, it is of considerable theoretical interest to examine whether for longer oligomers, several A_g-type states will make important contributions to the transverse TPA spectrum, or only one state (the transverse mA_g state) will eventually survive. The other interesting aspect is that whether the transverse mA_g state will owe its origins to the phenyl based orbitals as per Hückel model and SCI calculations, or will it emerge from the configurations interaction effects involving excitations among low-lying orbitals, as appears to be the case with the MRSDCI results on PDPA-5. These questions can only be answered by performing calculations on longer oligomers of PDPA's which we intend to pursue in future.

5 Acknowledgments

These calculations were performed on the Alpha workstations of Physics Department, and the Computer Center, IIT Bombay. We are grateful to Sumit Mazumdar (University of Arizona) for a critical reading of the manuscript, and for many suggestions for improvement.

References

[1] See, e.g., P.N Prasad and D.J. Williams, Introduction to Nonlinear Optical Effects in Molecules and Polymers, Wiley, New York, 1991.

[2] G.P. Agrawal, C. Cojan, and C. Flytzanis, Phys. Rev. B. 17 (1978) 776.

[3] S.N. Dixit, D. Guo, and S. Mazumdar, Phys. Rev. B 43 (1991) 6781.

[4] S. Mazumdar and F. Guo, J. Chem. Phys. 100 (1994) 1665.

[5] V.A. Shakin, S. Abe, and T. Kobayashi, Phys. Rev. B 53 (1996) 10656.

[6] A. Chakrabarti and S. Mazumdar, Phys. Rev. B 59 (1999) 4822.

[7] M. Y. Lavrentiev, W. Barford, S.J. Martin, H. Daly, and R.J. Bursill, Phys. Rev. B 59 (1999) 9987.

[8] A. Shukla, Phys. Rev. B 65 (2002) 125204.

[9] K. Tada, R. Hidayat, M. Hirohata, M. Teraguchi, T. Masuda and K. Yoshino, Jpn. J. Appl. Phys., part 2 35 (1996) L1138.

[10] K. Tada, R. Hidayat, M. Hirohata, H. Kajii, S. Tatsuhara, A. Fujii, M. Ozaki, M. Teraguchi, T. Masuda and K. Yoshino, Proc. SPIE-Int. Soc. Opt. Eng., 3145 (1997) 171.

[11] M. Liess, I. Gontia, T. Masuda, K. Yoshino, and Z.V. Vardeny, Proc. SPIE-Int. Soc. Opt. Eng., 3145 (1997) 179.

[12] A. Fujii, M. Shkunov, Z.V. Vardeny, K. Tada, K. Yoshino, M. Teraguchi and T. Masuda, Proc. SPIE-Int. Soc. Opt. Eng., 3145 (1997) 533.

[13] I. Gontia, S.V. Frolov, M. Liess, E. Ehrenfreund, Z.V. Vardeny, K. Tada, H. Kajii, R. Hidayat, A. Fujii, K. Yoshino, M. Teraguchi and T.Masuda, Phys. Rev. Lett. 82 (1999) 4058.

[14] R. Sun, Y. Wang, X. Zou, M. Fahlam, Q. Zheng, T. Kobayashi, T. Masuda and A.J. Epstein, Proc. SPIE-Int. Soc. Opt. Eng., 3476 (1998) 332.

[15] R. Hidayat, S. Tatsuhara, D.W. Kim, M. Ozaki, K. Yoshino, M. Teraguchi and T. Masuda, Phys. Rev. B 61 (2000) 10167.

[16] A. Fujii, R. Hidayat, T. Sonoda, T. Fujisawa, M. Ozaki, Z.V. Vardeny, M. Teraguchi, T. Masuda, and K. Yoshino, Synth. Met. 116 (2001) 95.

[17] A. Shukla and S. Mazumdar, Phys. Rev. Lett 83 (1999) 3944.

[18] H. Ghosh, A. Shukla, and S. Mazumdar, Phys. Rev. B 62 (2000) 12763.

[19] A. Shukla, H. Ghosh, and S. Mazumdar, Synth. Met. 116 (2001) 87.

[20] J. Yu and W.P. Su, Phys. Rev. B 44 (1991) 13315.

[21] Clearly, because of anisotropy, in these materials one can obtain longitudinal nonlinear optical response due to transversely polarized radiation also. However, such response, which will be possible due to the off-diagonal components such as $\chi^{(3)}_{xxyy}$ etc., will be much smaller.

[22] J. Yu, B. Friedman, P.R. Baldwin, and W.P. Su, Phys. Rev. B 39 (1989) 12814.

[23] K. Ohno, Theor. Chim. Acta 2 (1964) 219.

[24] M. Chandross and S. Mazumdar, Phys. Rev. B 55 (1997) 1497.

[25] A. Shukla, H. Ghosh, and S. Mazumdar, Phys. Rev. B 67 (2003) 245203.

[26] B.J Orr and J.F. Ward, Mol. Phys. 20 (1971) 513.

[27] The many-particle wave functions of half-filled conjugated polymers such as PDPA exhibit particle-hole (charge conjugation) symmetry when treated using the models such as the Hubbard model and the P-P-P model. Therefore, for every configuration which contributes to its wave function, its charge-conjugated (c.c.) counterpart will contribute in equal measure. For example, if configuration $|H \rightarrow L+1\rangle$ occurs in the wave function with coefficient 0.69, configuration $|H-1 \rightarrow L\rangle$ will also occur in the wave function with coefficient of the same magnitude (although, the sign could be reversed). Thus, we will use shorthand notation $|H \rightarrow L+1\rangle + c.c.$ (0.69) to denote the contribution of these configurations to the wave function.

[28] We are grateful to Sumit Mazumdar for bringing this point to our notice.